The potential formation of acid mine drainage in pyrite-bearing hard-coal tailings under water-saturated conditions: an experimental approach

J. Schüring · M. Kölling · H. D. Schulz

Abstract Annually, an amount of approximately 13 million cubic meters of hard-coal tailings must be disposed of in the German Ruhr Valley. Besides the waste of land in a densily populated region, the disposal of the pyrite-bearing material under atmospheric conditions may lead to the formation of acid mine drainage (AMD). Therefore, alternative disposal opportunities are of increasing importance, one of which being the use of tailings under water-saturated conditions, such as in backfilling of abandoned gravel pits or in the construction of waterways. In this case, the oxidation of pyrite, and hence the formation of AMD, is controlled by the amount of oxygen dissolved in the pore water of tailings deposited under water. In case the advective percolation of water is suppressed by sufficient compaction of the tailings, oxygen transport can be reduced to diffusive processes, which are limited by the diffusive flux of dissolved oxygen in equilibrium with the atmospheric pO_2. Calculations of the duration of pyrite oxidation based on laboratory experiments have shown that the reduction of oxygen is mainly controlled by the content of organic substance rather than the pyrite content, a fact that is supported by results from oxidation experiments with nitrate. A "worst case" study has lead to the result that the complete oxidation of a 1.5-m layer of hard-coal tailings deposited under water-saturated conditions would take as much as several hundred thousand years.

Key words Pyrite oxidation · Acid mine drainage · Tailings, landfill · Sealing · Modelling

Received: 6 May 1996 · Accepted: 2 August 1996

J. Schüring (✉) · M. Kölling · H. D. Schulz
FB 5 – Geowissenschaften, Universität Bremen,
Postfach 330440, D-28334 Bremen, Germany

Introduction

Due to the highly automated mining of hard-coal, the coal portion only amounts to some 50% of the total production of Germany's main hard-coal producer Ruhrkohle AG. Of the total production, 50% consist of tailings. In 1994, some 17 million cubic meters of the tailings had to be disposed of. A portion of 4 million cubic meters was used in the construction of waterways or refilling of sand and gravel pits; a few hundred thousand tons were re-cycled for backfilling of old shafts and some 13 million cubic meters had to be deposited on tailing heaps.

The chemical weathering of tailing heaps under atmospheric conditions is characterized by a time-dependent sequence of weathering processes (Schöpel and Thein 1991):

1. Mobilization of soluble salts (chloride, sulfate).
2. Oxidation of pyrite and subsequent buffering of the thereby formed acid by several buffering systems, ionic exchange of alkalines against alkaline earths.
3. Decrease of pH-values due to progressing pyrite oxidation and concurrent exhaustion of buffering systems.

The extent of the formation of AMD and the impact on the groundwater depends on the pyrite content and the oxidation rate which is controlled by the availability of oxygen as the oxidizing agent. Under atmospheric conditions, oxygen is readily available, whereas under water-saturated conditions only some 250 μmol/l are soluble.

The oxidation of pyrite by oxygen takes place in various steps, whereby the inorganic oxidation only plays a minor role (Taylor and others 1984; Moses and others 1987; Berk 1987; Kerth 1988).

The actual decomposition of pyrite takes place by ferric iron which is formed by the re-oxidation of ferrous iron.

$$FeS_2 + 14Fe^{3+} + 8H_2O \Leftrightarrow 15Fe^{2+} + 2SO_4^{2-} + 16H^+. \quad (1)$$

The re-oxidation of ferrous iron is microbially catalyzed mainly by several species of *Thiobazillus* bacteria the activity of which being the rate limiting step in pyrite oxidation.

$$Fe^{2+} + 1/4\,O_2 + H^+ \Leftrightarrow Fe^{3+} + 1/2\,H_2O. \quad (2)$$

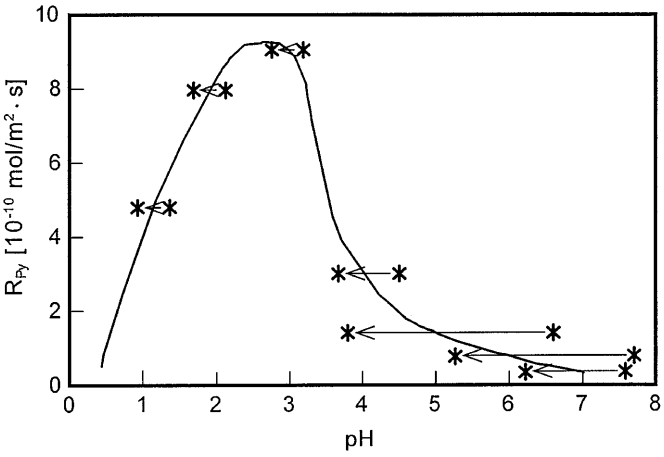

Fig. 1
Pyrite dissolution rates as determined by Kölling (1990). * = pH conditions after 1-hourly irrigations of a column filled with a sand/pyrite mixture. The *arrows* indicate the pH-decrease due to the formation of acid after irrigation

These organisms are tolerant to pH-values as low as pH = 0.5 and their spores are distributed via dust and aerosol deposition. Kölling (1990) determined the pH-dependent pyrite solution rates R_{Py} (Fig. 1). According to his study, the oxidation of pyrite occurs at a maximum rate between pH of 1 and 5. This is in accordance with results published by Beier (1982) who determined the upper limit of microbial activity at pH = 5. At pH < 1.8, the rate of pyrite oxidation decreases rapidly. The overall pyrite oxidation including the re-oxidation of ferrous iron takes place according to:

$$FeS_2 + 15/4O_2 + 7/2H_2O \Leftrightarrow Fe(OH)_3 + 2SO_4^{2-} + 4H^+. \quad (3)$$

The tailings investigated here contain various amounts of organic carbon C_{org} (see Table 1) which consists mainly of residual coal. In one sample, small amounts of flotation aids are to be expected, which mainly consist of various organic substances. These components do not play a role as a contaminant in water resources management (Leuchs 1991), but they may be more readily available for oxidation than the residual coal. During the process of aerobic respiration, organic carbon becomes oxidized according to:

$$CH_2O + O_2 \Leftrightarrow CO_2 + H_2O. \quad (4)$$

Table 1
Carbon and pyrite contents in the fraction ≤ 2 mm

	mC_{org} %	mC_{org} [mol/kg]	Pyrit-S %	$mFeS_2$ [mol/kg]
Hugo	12.55	10.45	0.1	0.02
Prosper	12.25	10.20	0.7	0.11

CH_2O is here used as a synonym for organic substance. It is obvious that the organic substance present in the hard coal tailings consists of various specific organic substances, such as residual hard coal and traces of flotation aids. Hence, the free energy change may be quite different. Depending on the quality of the organic substance as well as on the microbiological conditions, the processes of pyrite oxidation and decomposition of organic matter are in competion.

As a result of the mining process, the grain size distribution of the tailings is highly non-uniform, and hence the material can be compacted to a high extent. The hydraulic conductivity decreases with the degree of compaction, and when the fluid flow flux or Darcian velocity is ≤ 0.1 m/a, mechanical dispersion becomes insignificant (Shackelford 1991). Gillham and others (1984) showed that diffusion is dominant when the seepage velocity v_s is of the order of 0.005 m/a. For a clay liner, this seepage velocity corresponds to a saturated hydraulic conductivity of $k_f = 8 \cdot 10^{-11}$ m/s (porosity $\phi = 0.5$). When using the tailings as base sealing of landfills, German regulations require a saturated hydraulic conductivity of clay liners of $k_f \leq 5 \cdot 10^{-10}$ m/s (TA Abfall 1991). It is evident that diffusion is then the dominant process of migration.

It is possible to experimentally determine the diffusive flux, J, of dissolved oxygen into a given sample, which under stationary conditions can be described by Fick's first law.

$$J = -\phi \cdot D_e \cdot \frac{\partial C}{\partial z}, \quad (5)$$

where D_e is the effective diffusion coefficient, ϕ is the effective porosity, C is the oxygen concentration, t is time and z is transport distance.

If a steady-state profile of the oxygen concentration can be measured, it is possible to estimate the oxygen decomposition times and hence the extent of possible generation of acid mine drainage. Since the hydraulic conductivity in the compacted tailings is extremely low, the advective transport becomes negligible and it can be assumed that the oxidation front moves into the material solely by diffusion.

The oxygen flux was calculated based on an oxygen diffusion coefficient in free solution, $D_0 = 1.73$ cm²/d (at 20 °C), published by Lerman (1979). The effective diffusion coefficient D_e was derived from

$$D_e = \frac{D_0}{\theta^2}, \quad (6)$$

where the tortuosity, θ^2, was estimated by

$$\theta^2 = \phi \cdot F. \quad (7)$$

The formation factor F was empirically determined for a variety of sediments by Manheim (1970):

$$F = \phi^{-n} \quad (8)$$

For sands and sandstones with porosities less than 0.7, the exponent in Eq. 8 would be $n = 2$ ("Archie's Law").

Materials and methods

For the investigation of the diffusive oxygen transport in tailings under water-saturated conditions, samples of two coal mines were selected. The tailings of the mines Hugo in Gelsenkirchen-Buer and Prosper in Bottrop represent the rocks of the carbon-bearing Upper Carboniferous strata consisting mainly of clayey, fine-to-medium silty sandstones.

Structurally, the sediments are characterized by the coal mining process. During the coal refining process, a classification of the tailings takes place:

a) Fine fraction (up to 10 mm grain size),
b) coarse fraction (10–20 mm grain size),
c) flotation tailings (<0.75 mm grain size).

The unweathered tailings are mineralogically characterized by quartz, minor amounts of feldspar and carbonates, and the clay minerals illite, illite-smectite, kaolinite and chlorite (Wiggering 1993). Detailed investigations on the clay mineralogy of the tailings from the Hugo and Prosper mines were carried out by Schweisfurth (1996). The carbonate content is less than 1% in both samples, which is the reason for a low buffering capacity. In both cases, the carbonate content is not sufficient enough to potentially buffer the protons generated by the complete oxidation of the pyrite contained in the tailings (Schüring 1996).

Whereas the samples taken from the Prosper mine had only been in contact with water during coal extraction, the material derived from Hugo mine contained a portion of material which had undergone a flotation process. In this sample, it was therefore expected that some residual flotation aids were present. At the same time, the pyrite content of the Prosper sample (1.3 wt%; 0.11 mol/kg) was much higher than in the samples from Hugo (0.2 wt% or 0.02 mol/kg). The amounts of C-species and pyrite are listed in Table 1.

For the investigation of stationary oxygen concentration profiles, the fraction ≤ 10 mm was separated by wet sieving of the bulk material. The exposure of the material to the atmosphere was minimized by cool storage under water-saturated conditions in airtight containers.

The material was filled into 200-ml beakers and manually compacted. At the same time, water was added in order to maintain water saturation. Due to the high unconformity of the tailings, a bulk porosity of less than 0.2 was achieved. In interpreting diffusion experiments, the bulk porosity determined via the water content is generally assumed to be identical with the effective porosity. Rowe and others (1988) discussed this practice before the background that a certain portion of the pore space is not available for diffusive transport ("dead-end pores"). In addition to this, the exclusion of anions from the vicinity of the negatively charged clay surface may reduce the "effective porosity". On the bars of diffusion experiments with a clay till, Rowe and others (1988) were able to show that the porosity ϕ determined from the water content of the till appeared to provide a good indicator of the effective porosity.

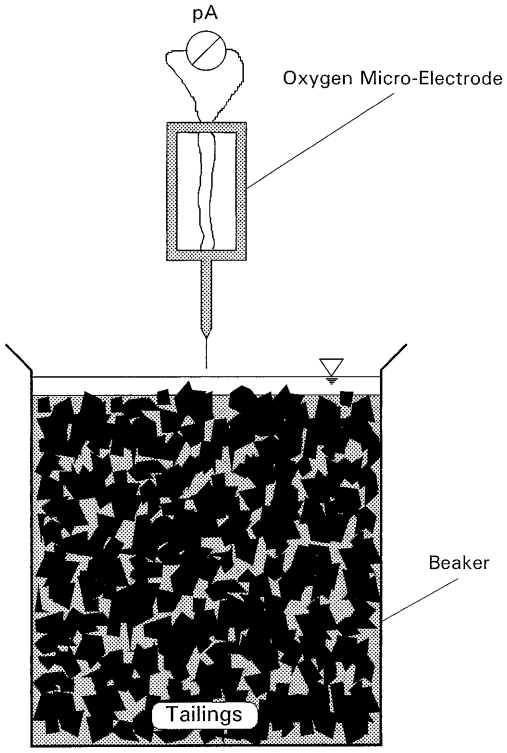

Fig. 2
Experimental setup for obtaining oxygen concentration profiles in tailings under water-saturated conditions

The experimental setup discussed in this paper is shown in Fig. 2. The water table on top of the sediment was approximately 1 cm above the sediment surface. This setup represents a system open to atmospheric oxygen. Thus, the water body on top of the sediment was saturated with respect to oxygen at all times. The exchange with atmospheric oxygen lead to a dissolved oxygen concentration of approximately 250 μmol/l, which was maintained by the equilibrium with pO_2.

The beakers containing the water-saturated tailings were left in a dark room for 7 days. After that time, the oxygen concentration in the pore water was measured by means of oxygen micro-electrodes fixed to a micro-manipulator allowing the electrodes to be driven into the sediment in steps of 25 μm (Revsbech 1989).

Results and discussion

The measured oxygen concentration profiles within the tailings of the mines Hugo and Prosper are shown as circles in Fig. 3. The curve labeled "No O_2-Consumption" represents the simulated depth profile of oxygen under the theoretical assumption that its diffusive transport behavior can be described as that of a conservative tracer. In this case, the oxygen concentration in the pore water would be near saturation at all depths. The measured

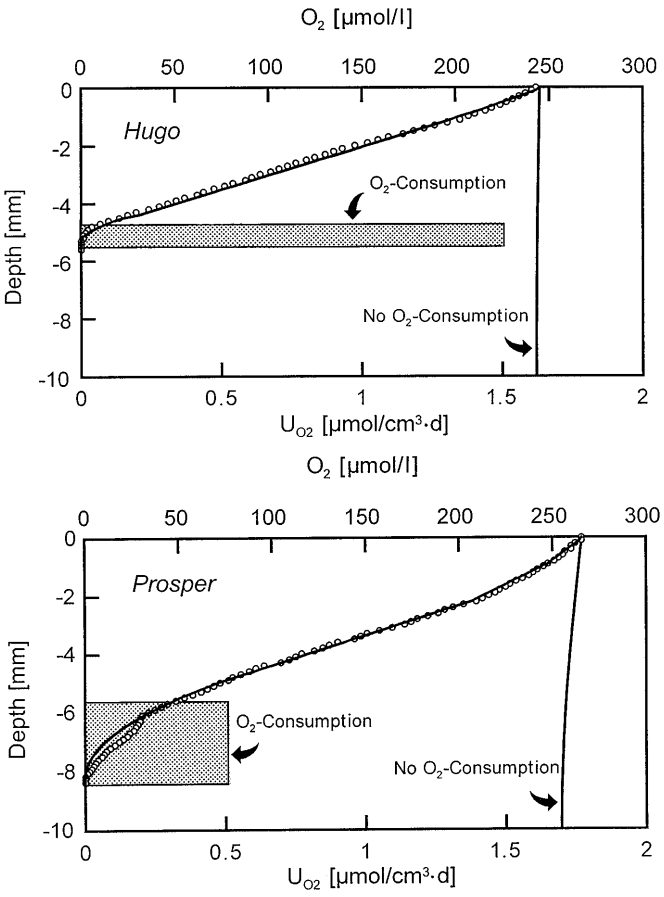

Fig. 3
Oxygen concentration profiles as measured by means of a microelectrode (*circles*). Oxygen consumption rates U_{O_2} (*bars*) were calculated on the base of fitted data (*solid curve*) with the program CoTAM (Hamer and Sieger 1994). The curves labelled "No O_2-Consumption" represent the theoretical depth profiles assuming that the diffusive transport of oxygen is that of an ideal tracer. The simulations represent the situation after 7 days during which the tailings were deposited under water-saturated conditions

steady-state profiles clearly show that oxygen is consumed by chemical reactions within the sediment.
The oxygen concentration profiles can be described by their gradients. Near the sediment surface the gradient is slightly flatter, which is the result of a slightly higher porosity due to continuing sedimentation of fine material suspended in the water body on top of the sediment. Below approximately 2 mm, both gradients become steeper and remain linear until they become flatter again when oxygen is consumed by chemical reactions. A qualitative description of the varying gradients is shown in Fig. 4. It illustrates that the consumption of oxygen takes place only in the vicinity of the penetration depth. Hence, the largely linear gradient may indicate that a steady state has been established. This state is reached when the diffusive flux of oxygen, J_{O_2}, is in equilibrium with the oxidative pyrite dissolution by oxygen D_{Py} (steady state):

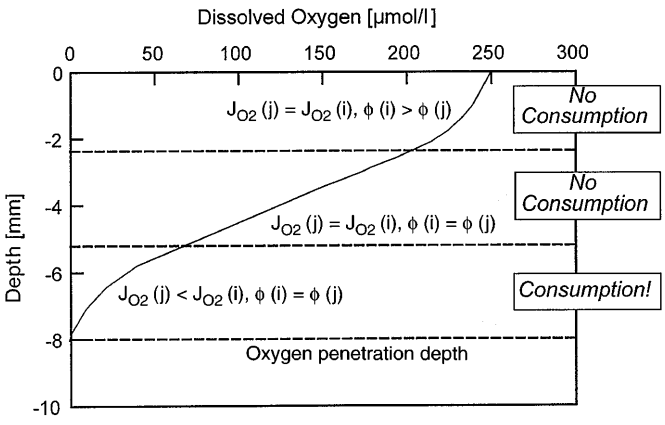

Fig. 4
Simplified description of the relationship between diffusive oxygen flux J_{O_2}, porosity ϕ and oxygen concentration versus a depth profile. The notations i and j represent discrete cells at a depth of $d(z)$ and $d(z+1)$, respectively

$$J_{O_2} = D_{Py},$$

where D_{Py} is expressed by the difference between the oxygen flux into cell i at a depth d(z) and the flux into cell j at a depth $d(z+1)$ (see Fig. 4).
At the time where a steady state has been established, the penetration velocity of oxygen into the sediment is controlled by the rate of the chemical reaction with oxygen and not by the diffusive velocity. Therefore, the concentration profile can be described by Fick's First Law (5).

The worst case: pyrite oxidation

It is obvious that the oxygen concentration profiles indicate by their different consumption rates that the oxygen penetration depth correlates with the quality of organic matter rather than the pyrite content. Thus, we can assume in a "worst case study" that the oxygen consumption is entirely due to the oxidation of pyrite. In that case, the complete amount of dissolved oxygen transported by diffusion would be available for the oxidation of pyrite. The oxidation of pyrite at least becomes important when the organic matter within the tailings is used up by oxidation.
The depth in which the stationary state is established can then be estimated with the help of pyrite weathering rates versus the diffusive flux of oxygen. For calculating the pyrite weathering rate, we have to estimate the reactive surface of pyrite, a_{Py}:

$$a_{Py} = \frac{\psi \cdot 6}{\rho_{Py} \cdot d_{Py}}, \qquad (9)$$

where ψ is the coefficient of roughness ($=10$), ρ_{Py} is the density of pyrite and d_{Py} is the particle diameter of pyrite.
The coefficient of roughness ψ is an empirical value which describes the deviation from an ideal circular and even surface of the pyrite particles. With an average grain size d_{Py} of 100 µm diameter and a coefficient of rough-

ness $\psi = 10$ the effective grain size is 10 μm (these numbers are estimated on the basis of electron microscopical investigation of the pyrite-bearing tailings). Together with the pyrite density, $\rho_{Py} = 5$ g/cm^3, the reactive pyrite surface is estimated to be 0.12 m^2/g. In a given volume of tailings, the reactive pyrite surface A_{Py} can be calculated as

$$A_{Py} = m_{Py} \cdot \rho_s \cdot a_{Py}, \quad (10)$$

where m_{Py} is the pyrite content in the tailing sample and ρ_s is the dry density of the sediment.
Corresponding to a pyrite content of 1.8 g/kg (0.02 mol/kg) in the Hugo sample and 13.1 g/kg (0.11 mol/kg) in the Prosper sample, the reactive pyrite surface within a cubic meter of tailings is: about 500 m^2 for Hugo and approximately 3600 m^2 for Prosper.
Assuming that the consumption of oxygen is completely attributed to the oxidation of pyrite, the depth-dependent oxygen consumption rate D_{Py} can be calculated with a pyrite weathering rate R_{Py} after Kölling (in: Vomberg 1994), where the factor 15/4 correlates to the stoichiometric reduction of oxygen by pyrite oxidation according to (3):

$$D_{Py} = 15/4 \cdot A_{Py} \cdot R_{Py} \cdot dz. \quad (11)$$

After fitting the experimental data (solid curve in Fig. 3), it is possible to compute the decomposition rates of oxygen. Hamer and Sieger (1994) developed the mathematical transport model CoTAM (Column Transport and Adsorption Model), which allows the fitting of experimental data on the basis of decomposition rates. The thus calculated oxygen consumption rates are shown as bars in Fig. 3. It is obvious that the total consumption rate has to be the same since the input oxygen concentration at the sediment/water interface in both experiments is approximately 250 μmol/l. Thus, the extent of oxygen consumption depends on its penetration depth. Therefore, the depth interval in which oxygen reduction takes place increases with the total penetration depth. Figure 3 shows that the oxygen consumption is higher in sample Hugo where it takes place within less than 1 mm, whereas in the Prosper sample the interval is almost 3 mm.
It is clear that the higher consumption rate in the Hugo sample does not correspond to its much lower pyrite content and, compared to the Prosper sample, slightly higher porosity. This without a doubt, indicates that the oxidation of pyrite is not the controlling parameter for the different oxygen concentration profiles. As mentioned above, the Hugo sample contains minor amounts of organic material in the form of flotation aids. It therefore seems to be very likely that the decomposition of oxygen is more controlled by the oxidation of organic matter, which is readily available in the Hugo sample, whereas it is less reactive in the Prosper sample. This is inaccordance with results from oxidation experiments with nitrate carried out by Schüring (1996).
Assuming that the oxygen consumption is entirely due to the oxidation of pyrite, the oxygen flux can be plotted versus the pyrite weathering rate. In Fig. 5, the diffusive

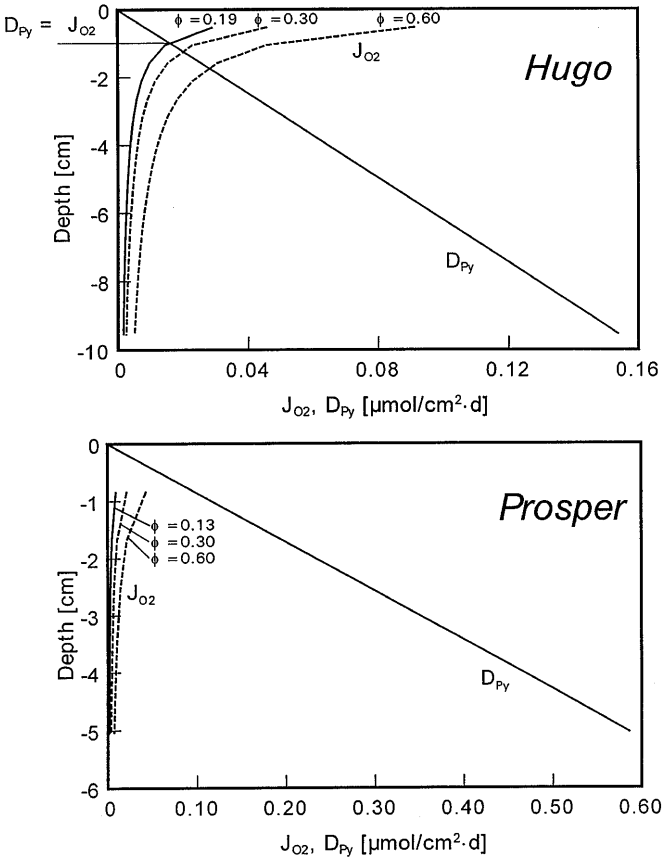

Fig. 5
Determination of the depth where oxygen consumption by pyrite oxidation D_{Py} is in the same order as diffusive oxygen flux J_{O_2} (the *solid line* is based on the total porosity ϕ in the experiment, whereas *dashed lines* were modelled on the basis of various porosities)

flux is plotted for several porosities. The solid line shows the water content (which is the effective porosity as discussed above) calculated volumetrically in the beakers. The curves of the Prosper sample indicate that the oxygen consumption at a depth of 8 mm is clearly controlled by the rate of pyrite oxidation, whereas in the Hugo sample the depth where D_{Py} equals J_{O_2} is at approximately 8 mm depth. The penetration depth of oxygen was determined as 5.2 mm. Thus an equilibrium was not quite reached.
Nevertheless, both profiles can be further investigated for the time needed to oxidize the pyrite contained in a given volume of tailings by diffusively transported oxygen. Even if equilibrium has not been established completely, the time needed for the oxygen transport to be controlled by the reaction rate is very short compared to the period of complete pyrite oxidation, because the diffusive oxygen gradient becomes flatter with increasing depyritization. Based on these considerations, a theoretical tailing layer of 1.5 m thickness was modelled, again with the assumption of various porosities. The whole thickness was subdivided in layers n with individual thicknesses d, which represents the oxygen penetration depth measured

in the experiments as shown in Fig. 3. For each cell $d(n)$ the time $t_{Ox}(n)$ needed to oxidize the whole amount of pyrite contained in that layer was estimated by

$$t_{Ox}(n) = \frac{m_{Py}(n) \cdot (1-\phi) \cdot d(n)}{J_{O_2}(n) \cdot 15/4} + t_{Ox}(n-1). \quad (12)$$

As mentioned above, it is legitimate to assume stationary states in interpreting both profiles, because the time of depyritization increases at the higher equilibrium depth $J_{O_2} = D_{Py}$. Hence, the calculations would even shift to greater time intervals. Also, this would only affect the time calculated for the upper few cells, which would hardly represent a few centimeters. Even in a "worst case" model assuming very low oxidation rates at high porosities and high grain size diameters, the equilibrium depth would shift to a maximum of 6 cm (Hugo) and 2 cm (Prosper), respectively (Fig. 6). Hence, the time needed for pyrite oxidation would increase. In case of the Hugo sample, the calculated oxidation timespan would be underestimated.

As shown above, the depth where equilibrium is reached between diffusive oxygen transport and pyrite oxidation rate varies within a few centimeters only. Steady states can be assumed when calculating the depyritization time of a 1.5-m-thick layer of compacted tailings. The expected timespans for varying porosities are plotted in Fig. 7. It is certain that the complete oxidation of pyrite in a water-saturated tailings heap would take place over at least a couple of ten thousand years. For the measured low porosities which can be achieved by compaction, several hundred thousand years may be expected. This modelling does not take into account that pyrite weathering rates decrease again at low pH-values (see Fig. 1), which will probably establish within the reaction rim, again leading to an extension of the depyritization time.

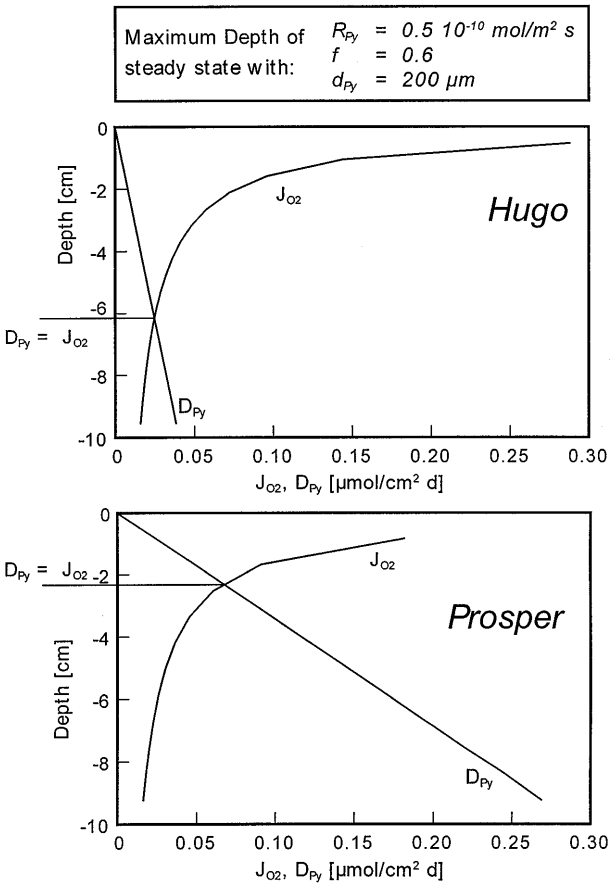

Fig. 6
Calculation of the maximum depth of steady state between oxygen consumption by pyrite oxidation D_{Py} and diffusive oxygen flux J_{O_2}

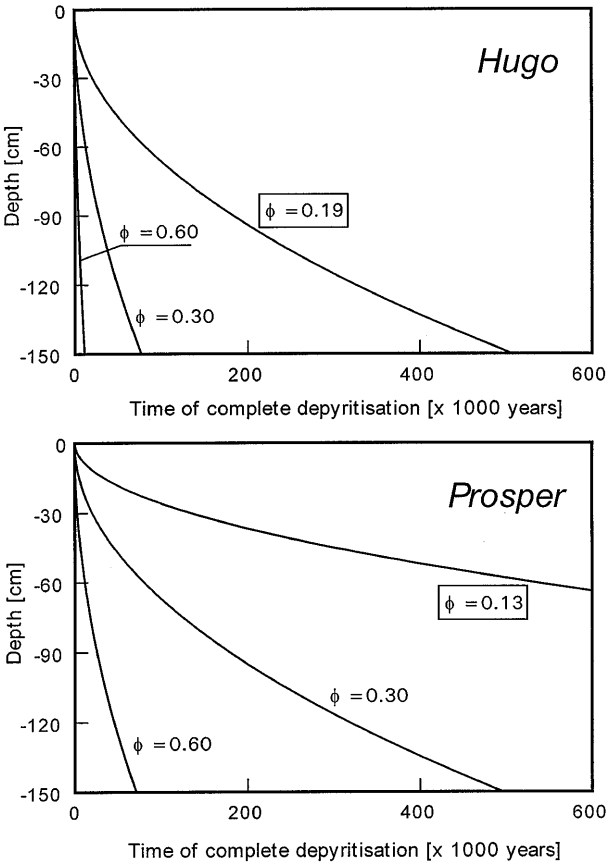

Fig. 7
Calculation of the time needed for complete depyritization of 1.5-m-thick tailings with various porosities, assuming that oxygen is entirely used up by pyrite oxidation. The marked porosities are as measured in the experiment

Conclusions

The experiments described, together with the modelling of this scenario, have shown that the oxidation of pyrite by dissolved oxygen under water-saturated conditions is clearly limited by the oxygen available by diffusive transport. The equilibrium between the pyrite oxidation rate

and the diffusive oxygen flux is established after a few days or weeks. From that time the diffusive flux of oxygen is the rate-limiting step. With increasing depth of depyritization the gradient of the diffusive oxygen flux flattens, and hence the progression of the oxidation front slows down exponentially. The modelling of this scenario is even based on the assumption of uniform oxidation rates, although the pH is expected to drop to very low values, since the natural buffering capacity of the tailings is low. In that case, oxidation rates would decrease significantly, and the oxidation may even stop completely. Summarizing our investigations, we conclude that pyrite oxidation is negligible once the pyrite-bearing material is deposited under water-saturated conditions. From the point of view of formation of acid mine drainage the deposition of hard-coal tailings under water-saturated conditions may lead to new options for the disposal of hard-coal tailings such as in the construction of waterways, the backfilling of sand and gravel pits or as base sealing in landfills.

Acknowledgements we wish to thank Ruhrkohle Montalith GmbH for funding this project.

References

Beier E (1982) Unerwünschte und gezielte Oxidation von Pyrit, insbesondere von Pyrit in der Kohle. Glueckauf Forschungsh 43:132–134

Berk W van (1987) Hydrochemische Stoffumsetzungen in einem Grundwasserleiter – beeinflußt durch eine Steinkohlenbergehalde. Bes Mitt Dtsch Gewässerkd Jahrb 49:175

Gillham RW, Robin MLJ, Dytynyshyn DJ, and Johnston HM (1984) Diffusion of nonreactive and reactive solutes through fine-grained barrier materials. Can Geotech J 21:541–550

Hamer K and Sieger R (1994) Anwendung des Modells CoTAM zur Simulation von Stofftransport und geochemischen Reaktionen. Berlin: Ernst & Sohn Verlag, pp 186

Kerth M (1988) Die Pyritverwitterung im Steinkohlenbergematerial und ihre umweltgeologischen Folgen. Diss Univ Essen, pp 182

Kölling M (1990) Modellierung geochemischer Prozesse im Sickerwasser und Grundwasser. Ber Fachbereich Geowiss Univ Bremen 8. pp 135

Lerman A (1979) Geochemical Processes Water and Sediment Environments. John Wiley, pp 481

Leuchs W (1991) Wasserwirtschaftliche Anforderungen an die Verwertung von Reststoffen im Erd- und Straßenbau. Gewässerschutz – Wasser – Abfall 131:651–684

Manheim FT (1970) The diffusion of ions in unconsolidated sediments. Earth Planet Sci Lett 6:114–186

Moses CO, Nordstrom DK, Herman JS, and Mills AL (1987) Aqueous pyrite oxidation by dissolved oxygen and by ferric iron. Geochim Cosmochim Acta 51:1561–1571

Revsbech NP (1989) An oxygen microelectrode with a guard cathode. Limnol Oceanogr 34:474–478

Rowe RK, Caers CJ, and Barone F (1988) Laboratory determination of diffusion and distribution coefficients of contaminants using undisturbed clayey soll. Can Geotech J 25:108–118

Schöpel M and Thein J (1991) Stoffaustrag aus Bergehalden. In: Wiggering H, Kerth M (Eds), Bergehalden des Steinkohlenbergbaus. Wiesbaden: Vieweg, 115–128

Schüring J (1996) Die Verwendung von Steinkohlebergematerialien im Deponiebau im Hinblick auf die Pyritverwitterung und die Eignung als geochemische Barriere. Ber Fachbereich Geowiss, Univ Bremen 75:pp 110

Schweisfurth M (1996) Die Verwendung von Steinkohlebergematerialien im Deponiebau im Hinblick auf das geochemische Verhalten gegenüber organischen Prüfflüssigkeiten und die Eignung als geochemische Barriere. Diss Univ Essen, pp 149

Shackelford CD (1991) Laboratory diffusion testing for waste disposal – A review. J Contam Hydrol 7:177–217

TA Abfall (1991) Zweite Allgemeine Verwaltungsvorschrift zum Abfallgesetz: Technische Anleitung zur Lagerung, chemisch/physikalischen, biologischen Behandlung, Verbrennung und Ablagerung von besonders überwachungsbedürftigen Abfällen. In: Abfallgesetz mit Verordnungen, Verwaltungsvorschriften und sonstigen einschlägigen Regelungen (1994). München: C. H. Beck, pp 123–247

Taylor, BE, Wheller MC, and Nordstrom DK (1984) Stable isotope geochemistry of acid mine drainage: Experimental oxidation of pyrite. Geochim Cosmochim Acta 48:2669–2678

Vomberg S (1994) Einsatz von Bergematerial im Tiefbau – Untersuchungen zum Verwitterungsverhalten von in Straßendämmen und Kanaldeichen eingebautem Bergematerial des Niederrheinisch-Westfälischen Steinkohlenbergbaus im Hinblick auf dessen wasserwirtschaftliche Bedeutung. Diss Techn Univ Clausthal, pp 288

Wiggering H (1993) Einsatz von Bergbaureststoffen bei der Abfalldeponierung – Beispiel: Reststoffe des Steinkohlenbergbaus. In: Dörhöfer G, Thein J, Wiggering H (Eds), Abfallbeseitigung und Deponien. Schriftenr Umweltgeol Heute 1:33–40